Available online at www.sciencedirect.com
SCIENCE DIRECT®
Ocean Engineering 31 (2004) 2253–2282
OCEAN ENGINEERING
www.elsevier.com/locate/oceaneng

Wave resistance for high-speed catamarans

H.B. Moraes [a], J.M. Vasconcellos [b,*], R.G. Latorre [c]

[a] *Pará University, CEP 66075-110, Brazil*
[b] *Naval Architecture Department, Federal University of Rio de Janeiro, COPPE/UFRJ, Bloco I, apt.1002, Rua Conde de Bonfim 850, Rio de Janeiro, Brazil*
[c] *University of New Orleans, LA 70148, USA*

Received 7 November 2003; accepted 31 March 2004

Abstract

The object of this study was to investigate the wave resistance component for high-speed *catamarans*. Two methods were applied: the slender-body theory proposed by Michell [Philos. Mag. 45(5) (1898) 106] and a 3D method used by Shipflow® (FLOWTECH, Shipflow® 2.4, User Manual, 1988) software.

Results were obtained for different types of twin hulls and attention was given to the effects of catamaran hull spacing.

The study also included the effects of shallow water on the wave resistance component.

Special attention was given to the height of waves generated by the craft to ascertain effects on river banks.

Keywords: Wave resistance; Catamaran design; Catamaran resistance; High-speed vessels

1. Introduction

The demand for high-speed passenger craft, mainly catamarans, has been increasing significantly in recent years. In order to meet this growing demand, the international market for high-speed craft is undergoing far-reaching change.

Different types of craft are being used for passenger transportation. However, the catamarans and monohulls have been the main shipowner's choice not only for passenger transportation but also as ferryboats. Research into more efficient

* Corresponding author.
E-mail address: jmarcio@peno.coppe.ufrj.br (J.M. Vasconcellos).

0029-8018/$ - see front matter © 2004 Published by Elsevier Ltd.
doi:10.1016/j.oceaneng.2004.03.012

hydrodynamic shapes, engine improvements and lighter hulls employing aluminum and composite materials has been made for higher speeds.

The demand for catamarans is justified to a point by improved craft quality, high speeds and larger deck area as compared with monohull craft.

The market for high-speed craft demands catamarans of different types and dimensions, designed for lower resistance and powered for high speed. Optimization of hull resistance is thus fundamental to the success of a high-speed catamaran hull.

The theoretical calculation of hull resistance is complex, but less costly than model test evaluation. This justifies the effort involved in studying many different theoretical methods in order to evaluate hull resistance properly.

This study focuses on two methods for calculating catamaran wave resistance under different conditions of hull separation and water depth: the 3D method based on the potential theory, used in the Shipflow™ (FLOWTECH, 1988; Nishimoto, 1998; Dawson, 1977; Picanço, 1999; Havelock, 1934) software and the method using slender-body theory (Williams, 1994), which is easier to apply.

The Shipflow™ program allowed a large number of analyses to be made of catamaran hull wave resistance. Particularly important was that the interference effect between hulls and the effect of shallow water could be studied.

This study also considered the maximum height of waves generated by the craft in different depths of water. The intention is to evaluate and minimize the possible effects on the river shore and/or on nearby small boats (Doctors, 1991).

2. High-speed craft

High-speed craft have always been at the forefront of naval engineering and *hydrodynamic* research.

In the late 19th and early 20th centuries, many solutions were encountered for alternatives types of high-speed craft, and many concepts were patented.

The first hydrofoil, built by Forlanini in 1905, achieved 61 knots. However, it was Baron Schertei who, between 1920 and 1930, developed the hydrofoil from a craft created to work in calm waters to one able to operate in ocean-going conditions.

High-speed craft can be classified as shown in Table 1.

International Maritime Organization (IMO) rules and recommendations, set out in IMO-HSC (high-speed craft) (IMO-HSC, 1995) special code approved by the

Table 1
Classification of types of high-speed craft

Category	Types of craft
Craft supported by air	Air-Cushion Vehicle (ACVs) and Surface-Effect Ship (SES)
Craft supported by foils	Surface-Piercing Foil (Hydrofoil) and Jetfoil
Displacement, planing and semi-displacement craft	Standard monohull, catamaran, Small Waterline Area Twin Hull (SWATH), Air-lubricated and Wave Piercing hulls

63rd section in May 94 through MSC.36 (63), specify a high-speed craft as one whose maximum speed is equal or superior to:

$$V = 3.7 \times \mathrm{Vol}^{0.1667} \ (\mathrm{m/s}) \tag{1}$$

where "Vol" is the displacement volume at design water line (m^3).

Fig. 1 shows the speed limit curve for a craft to be considered as a high-speed craft.

Catamaran hydrodynamic performance depends on the wetted geometrical forms, hull separation and water depth where the craft is going to sail.

3. Hull resistance evaluation methods: comparison of results

Results obtained from Shipflow™ (1988) and the slender-body theory application were compared with the Millward (1992) study of the effects of catamaran hull separation and shallow water in a wide Froude number range (Hess and Smith, 1964; Newman, 1977; Lunde, 1951; Everest, 1968; Kostjukov, 1977; Insel and Molland, 1991).

The Millward (1992) results can be compared with catamaran hulls in the following range:

length/breadth $(L/b) \Rightarrow 6.00–12.00$;
breadth/draught $(b/T) \Rightarrow 1.00–3.00$;
block coefficient $\Rightarrow 0.33–0.45$;
Froude number $\Rightarrow 0 < Fn < 1$.

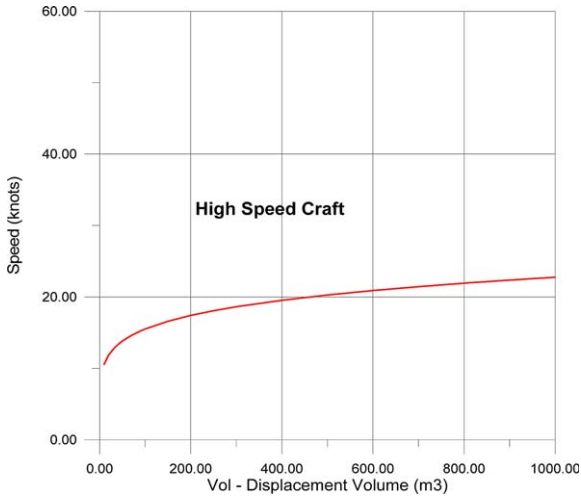

Fig. 1. Speed limit for high-speed craft.

3.1. Hull geometry

Two hull geometries were used to compare wave resistance calculation methods. The first utilized the mathematical model proposed by Wigley (1942) (Fig. 2) and the second is a chine hull as indicated in Fig. 3.

The parabolic hull proposed by Wigley (1942) has already been subjected to exhaustive theoretical tests and experiments, and is thus well known and tested. The hull geometry in a no-*dimensional* form of the Wigley hull is given by the equation:

$$Y = \left[\pm\frac{1}{2}b(1-4x^2)\left(1-\frac{z^2}{d^2}\right)\right] \quad -\frac{1}{2}\le x\le\frac{1}{2},\ -d\ \le z\le 0 \tag{2}$$

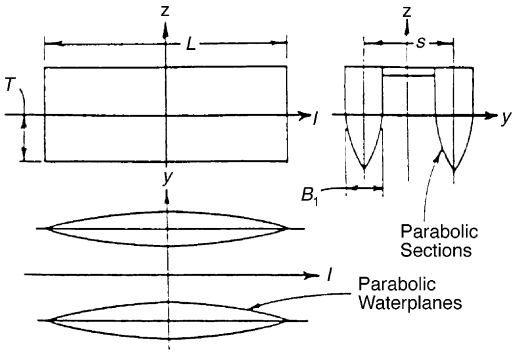

Fig. 2. Wigley catamaran hull.

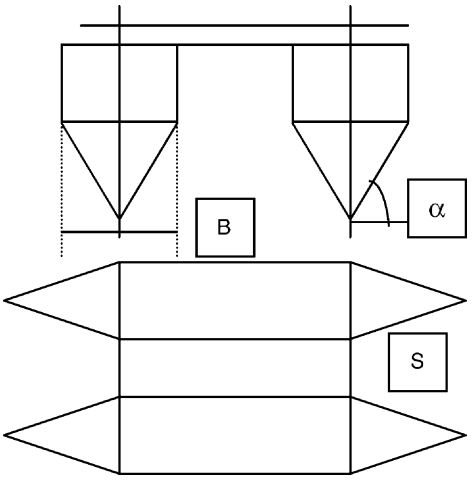

Fig. 3. Catamaran chine hull.

where b and d are constants ($b = 0.1$ and $d = 0.0625$).

$$b = \frac{b}{L} \tag{3}$$

$$d = \frac{T}{L} \tag{4}$$

where L is the length; B the breadth and T the draught.

The chine hull catamaran form is defined by straight water lines forming a triangle in the fore body, a parallel central body in the form of a rectangle and an after body with triangular or rectangular form, when a transom is considered. The hull section has a "V" shape geometry (Fig. 3).

An algorithm was developed in FORTRAN℠ to generate the chine hull. The hull is created following the range constraints:

$S/L \Rightarrow 0.2 \leq S/L \leq 1.0$;
$b/T \Rightarrow 10 \leq b/T \leq 16$;
deadrise angle (degrees) 25°;
entrance body length 0.3 L;
exit body length 0.3 L;

where S is the distance between hulls (m); L the craft's length (m); B the breadth (m) and T the craft's draught (m).

The catamaran hull geometry generated by the Fortran program output the hull data in a standard format for the Shipflow℠ program and the slender-body program, which calculated wave resistance (Fig. 4).

3.2. Wigley's hull results

Wave coefficient (C_w) was used to compare the catamaran wave resistance results given by the Shipflow℠ and SLENDER (slender-body theory) programs (Williams,

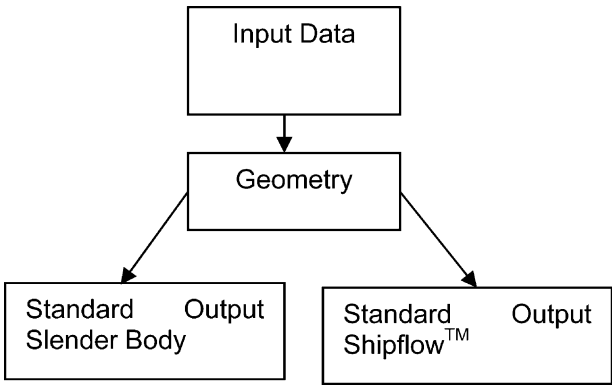

Fig. 4. Flow chart of the algorithmic form generator.

1994). The Wigley hull was tested in deep water for three different hull separations ($S/L = 0.2$, 0.4 and 1.0), where S is the distance between hull centers and L is hull length.

The results for a captive hull (in relation to the water surface) are presented in Figs. 5–7.

The methods show similar trade-off results. The 3D method used by the Shipflow™ program and the slender-body theory gave different results for Froude numbers between 0.5 and 0.7. The difference can be explained by the fact that the Shipflow™ program applies a 3D method and takes account of the stronger hull interference in this Froude range, while Millward (1992) and the Slender program use a similar methodology (2D).

The results highlight a substantial increase in the wave resistance coefficient when the hull separation is small, showing the hull interference effect. Figs. 5–7 point to the following conclusions:

At small S/L, the differences between the results given by the Shipflow™ and Slender programs increase.
For $0.2 \leq Fn \leq 0.4$ and $Fn > 0.8$, the results given by the Shipflow™ and Slender programs are very close to those of Millward (1992), confirming the accuracy of all these methods for this Froude range.
At Froude numbers higher than 0.8, the C_w value converges at around 0.0002 for all the S/L ratios observed (0.2, 0.4 and 1.0).

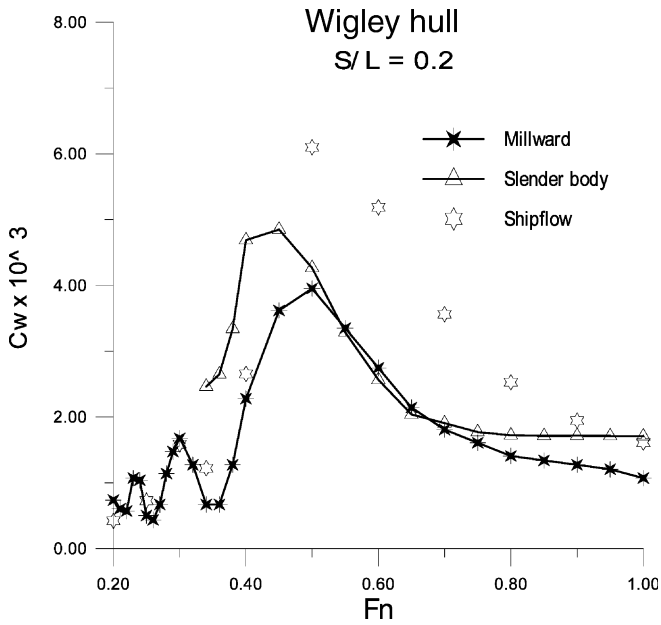

Fig. 5. Wave coefficient (C_w)—Wigley case—catamaran ($S/L = 0.2$).

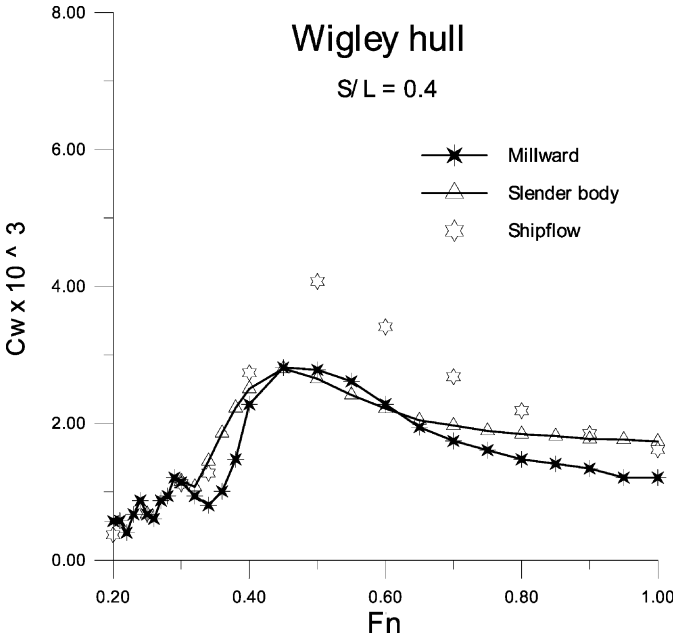

Fig. 6. Wave coefficient (C_w)—Wigley case—catamaran ($S/L = 0.4$).

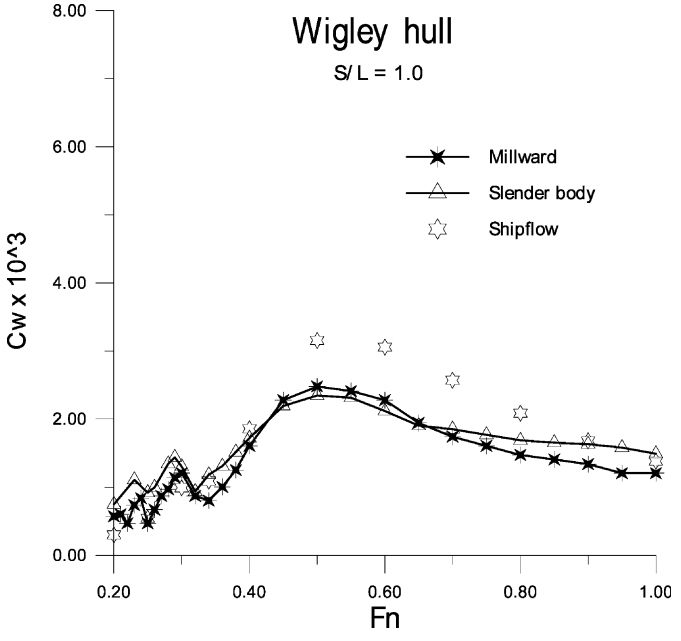

Fig. 7. Wave coefficient (C_w)—Wigley case—catamaran ($S/L = 1.0$).

The smaller the spacing between the twin hulls, the higher is the C_w curve for Froude numbers around 0.5.

Regarding the previous results obtained with a captive hull in relation to the water surface, the Shipflow™ program was used with the hull in a free condition to determine the C_w curve trade-off, the variation in underwater hull volume and the wetted surface area for different Froude numbers.

Figs. 8 and 9 show and compare the results for the Wigley monohull in captive and free conditions and in shallow and deep water ($L/h = 5$; $L =$ length, $h =$ depth) (Millward and Sproston, 1988).

Results indicate considerable differences in the C_w values for Froude numbers between 0.3 and 0.6 for the monohull free and captive in relation to the water surface. These differences are even greater when the depth effect is included. When the sea or river bottom is close to the hull, the craft's draft is increased and consequently displacement and wetted surface area are increased.

The same tests were conducted for twin hull craft. Figs. 10–12 show the results for the Wigley catamaran hull for different twin hull spacing (S/L) and depths in a free condition.

When Figs. 10–12 are compared with Figs. 5–9, it can be seen that, with monohulls, there is a tendency to higher C_w values in the free condition at Froude numbers between 0.3 and 0.6. With catamarans, this effect is even greater when the hull separation is small, an effect that is increased when the shallow water effect occurs. Results at Froude numbers greater than 0.7 show that the C_w values are basically

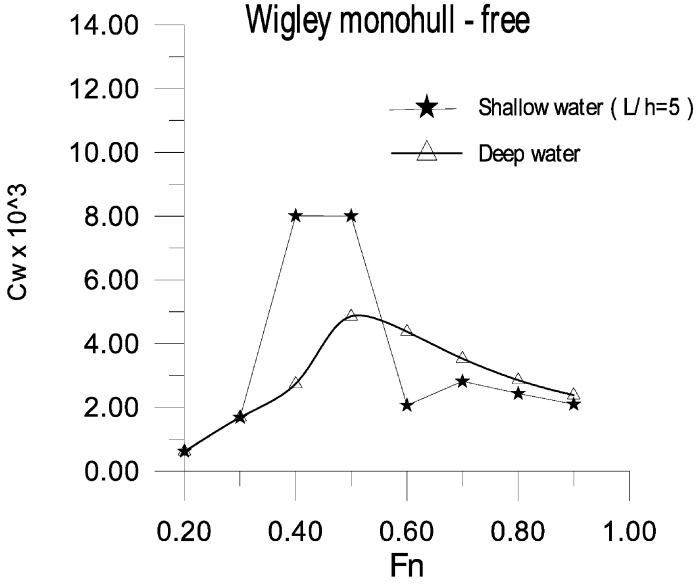

Fig. 8. C_w coefficient for monohull in free condition.

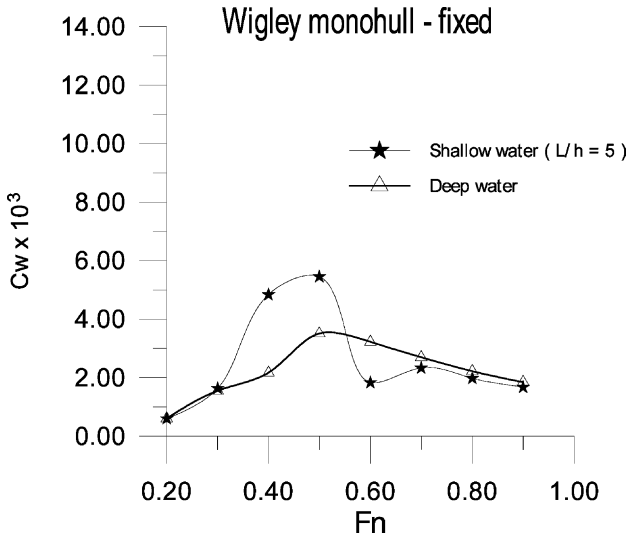

Fig. 9. Monohull C_w coefficient in captive condition.

the same for monohulls and catamarans, leading us to conclude that hull separation does not matter. For Froude numbers greater than 0.7, hull interference is practically absent and catamaran wave resistance can be calculated as twice the monohull resistance.

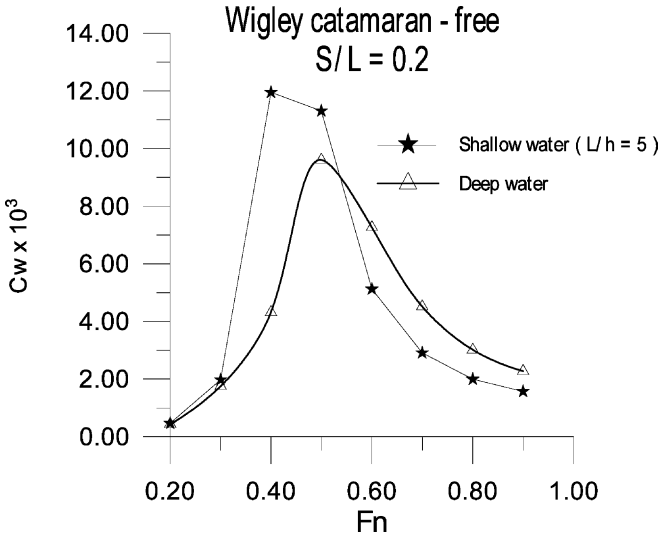

Fig. 10. Wigley catamaran—C_w coefficient in a free condition and $S/L = 0.2$.

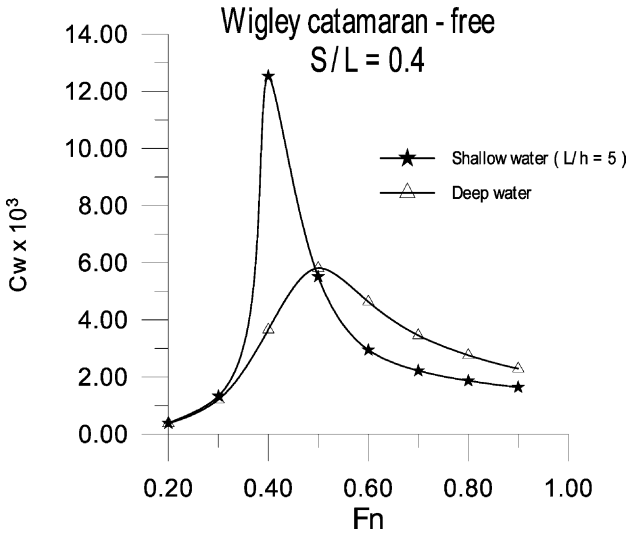

Fig. 11. Wigley catamaran C_w coefficient in a free condition and $S/L = 0.4$.

In the foregoing figures, C_w coefficients at Froude numbers between 0.3 and 0.6 are greater in the free case. This results from the sinkage of the hull.

Figs. 13–20 show an increased percentage of underwater volume and wetted hull surface area for monohull and catamaran. Under free hull conditions, monohull

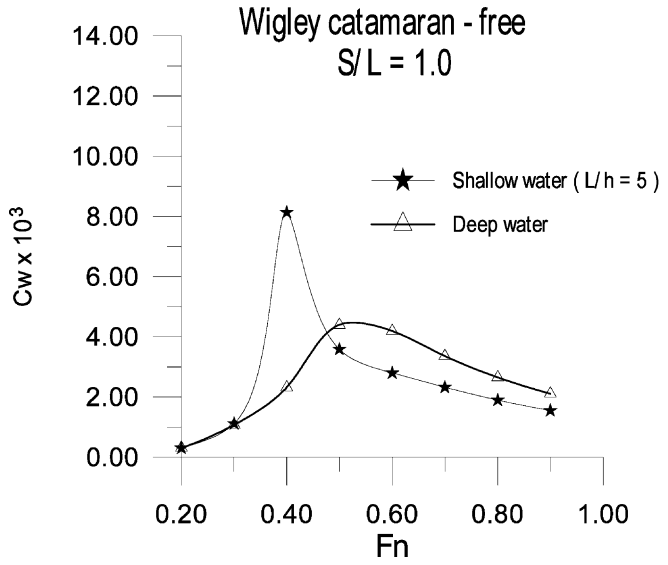

Fig. 12. Wigley catamaran—C_w coefficient in a free condition and $S/L = 1.0$.

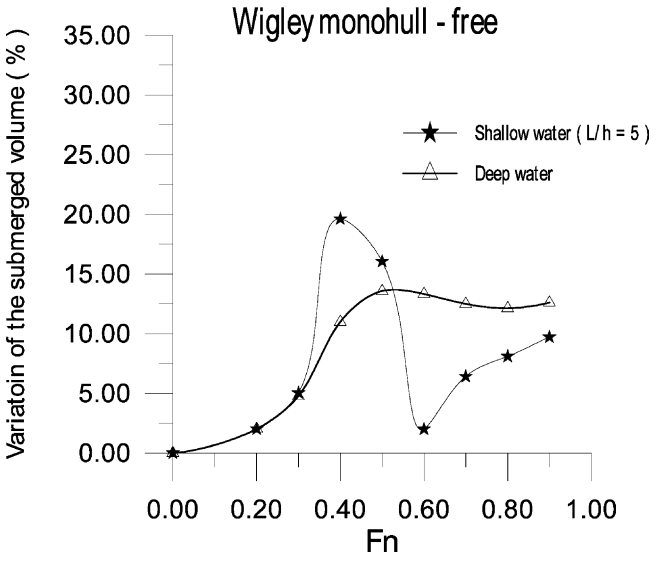

Fig. 13. Monohull volume variation in free condition.

volume increases approximately 12% in deep water and 20% in shallow water ($L/h = 5$).

In catamarans, this effect is enhanced by hull interference, as can be seen in the graphs in Figs. 14–16. Fig. 14 shows an increase of 33% in volume in shallow water when the twin hull separation is 0.2 (S/L) and Froude numbers between 0.3 and

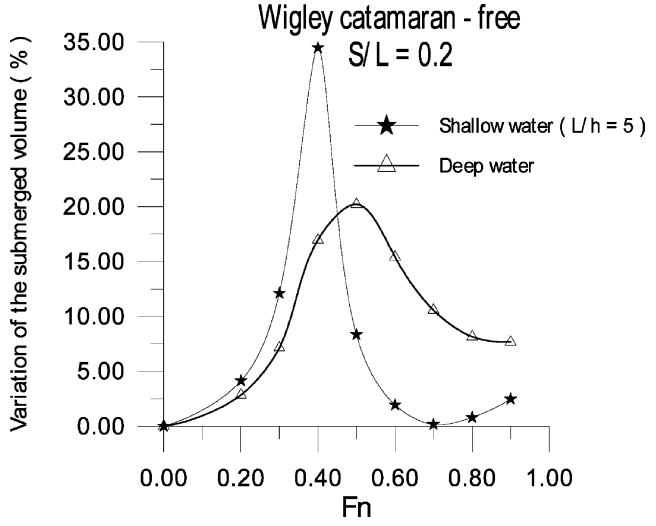

Fig. 14. Catamaran volume variation in free condition and $S/L = 0.2$.

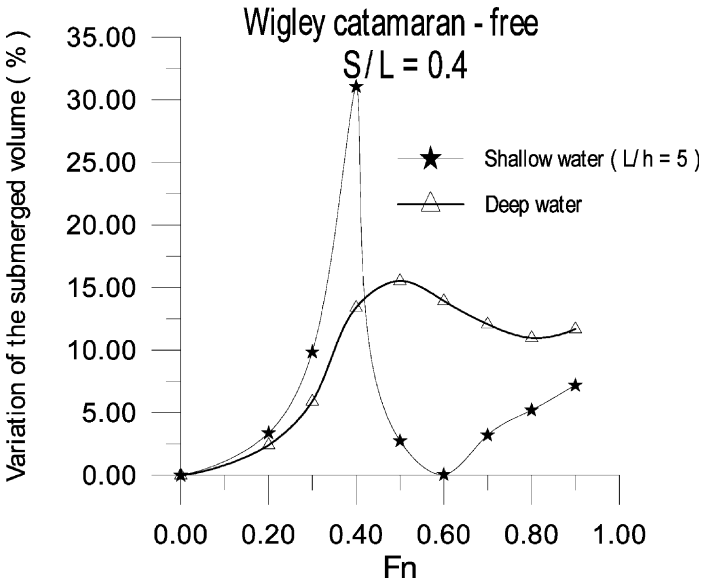

Fig. 15. Catamaran volume variation in free condition and $S/L = 0.4$.

0.5. It also shows that for deep water the C_w curve reaches a peak at around 0.5, and the peak shifts for Froude numbers around 0.4 when the shallow water effect occurs.

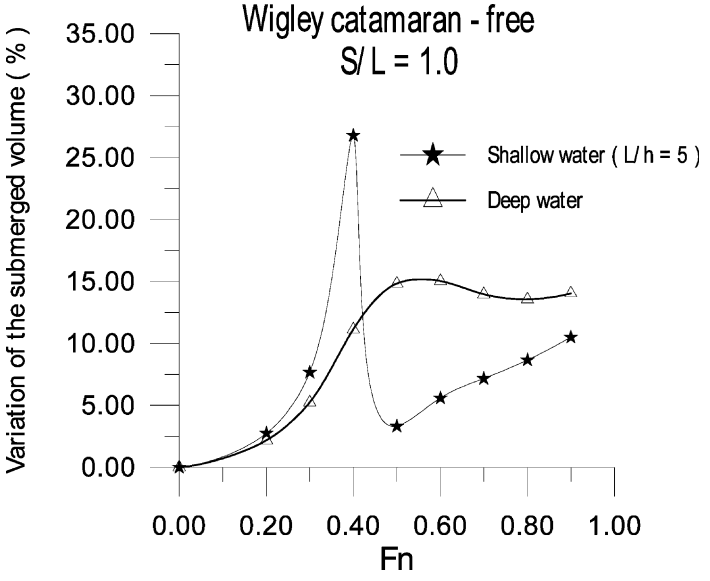

Fig. 16. Catamaran volume variation in free condition and $S/L = 1.0$.

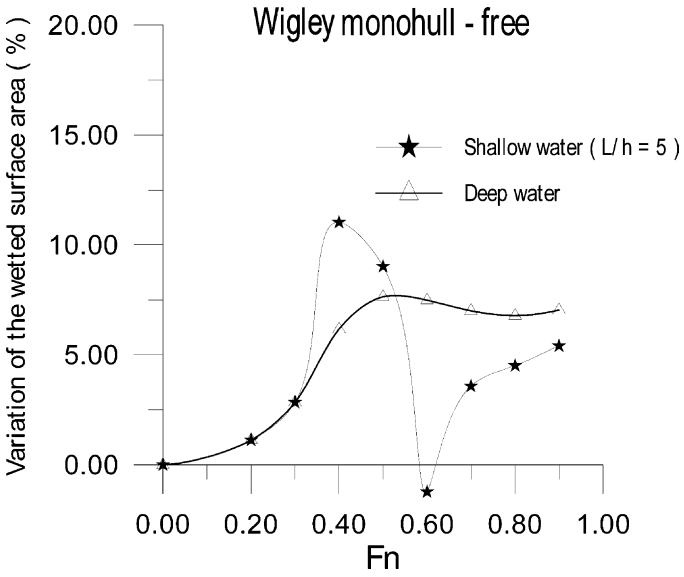

Fig. 17. Monohull wetted surface area variation in free condition.

The same effect that occurs with volume also occurs with the wetted surface, with a smaller percentage increase, however, of around 19% in the most critical condition (shallow water and $S/L = 0.2$) (Fig. 18).

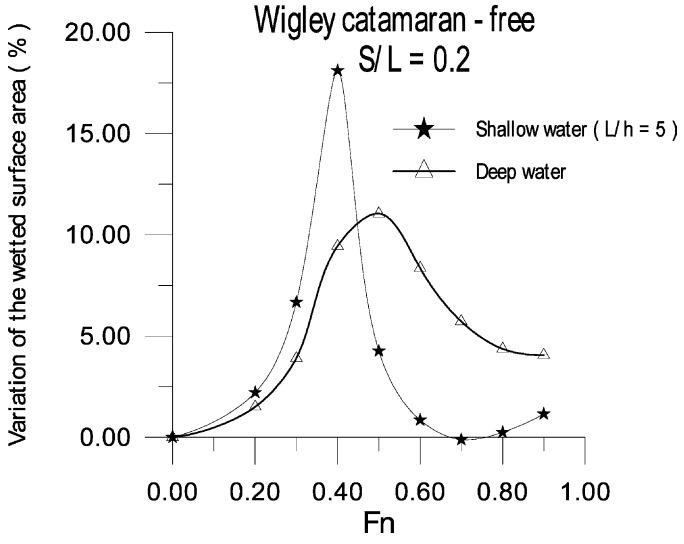

Fig. 18. Catamaran wetted surface area variation in free condition and $S/L = 0.2$.

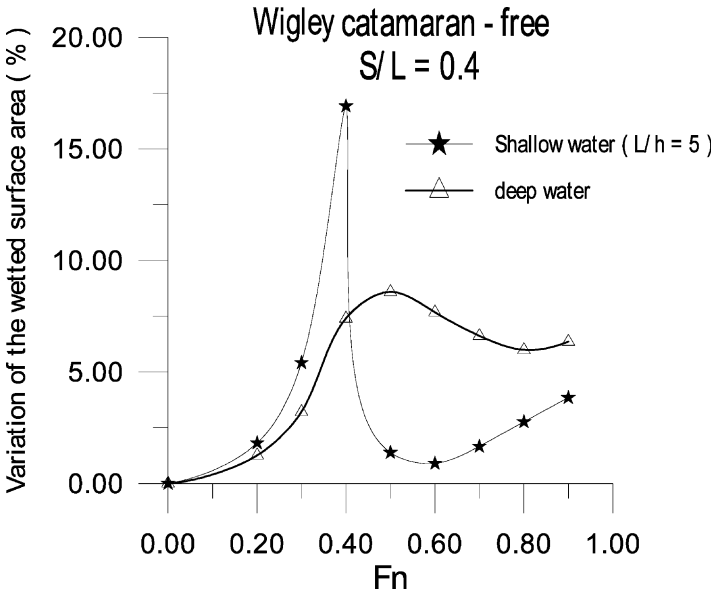

Fig. 19. Catamaran wetted surface area variation in free condition and $S/L = 0.4$.

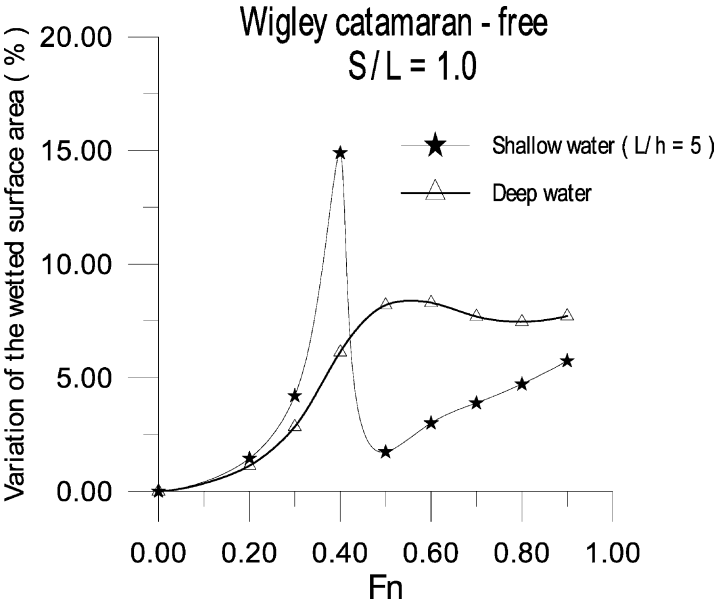

Fig. 20. Catamaran wetted surface area variation in free condition and $S/L = 1.0$.

4. Catamaran chine hull results

Chengyi (1994) shows that the shape of symmetrical catamaran hulls has little influence on catamaran wave resistance. To investigate different catamaran chine hull geometries (effects of hull separation and water depth) with the Shipflow™ program, an algorithm was used that quickly and effortlessly modifies the geometric forms of the hull.

The hull generated for analysis has the following characteristics:

length (L): 40 m;
breadth (b): 3.5 m;
draft (T): 1.5 m;
deadrise angle (A): 25°.

Wave resistance data were obtained using the program Shipflow™ at the same twin hull separations and water depths analyzed in Millward (1992).

The nomenclature used in the variables was defined according to the outlines in Figs. 21 and 22.

The results are analyzed by to the Froude numbers (Fn) and speeds (V) shown in Table 2.

Figs. 23–25 show the main results obtained by the Shipflow™ program for a chine hull catamaran in the free condition.

Figs. 23–25 support the following conclusions:

Critical C_w (C_w curve peak) tends to increase with decreasing water depth. Also, hull interference was observed to remain practically unchanged at Froude numbers higher than 0.7 in any depth of water.

In shallow water, the peak of C_w curve is close to Froude number 0.4.

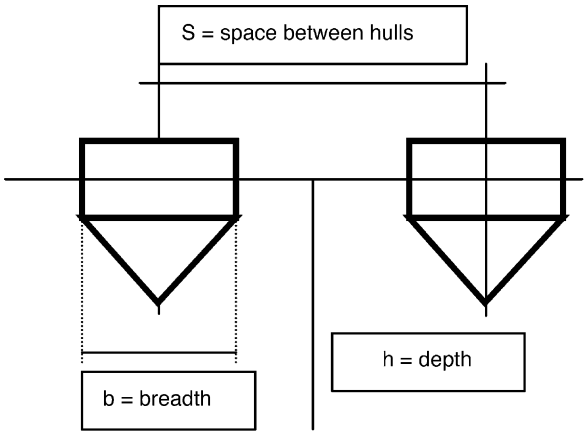

Fig. 21. Forty-meter catamaran hull section.

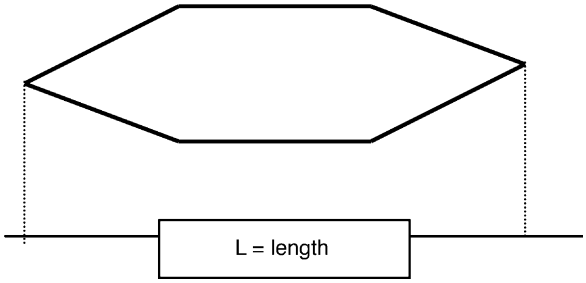

Fig. 22. Waterline shape.

Table 2
Froude number and speed for a 40-m chine hull catamaran

Fn	*V* (m/s)	*V* (knots)
0.2	3.96	7.70
0.3	5.94	11.54
0.4	7.92	15.39
0.5	9.90	19.24
0.6	11.90	23.12
0.7	13.86	26.93
0.8	15.84	30.78
0.9	17.82	34.62
1.0	19.80	38.48

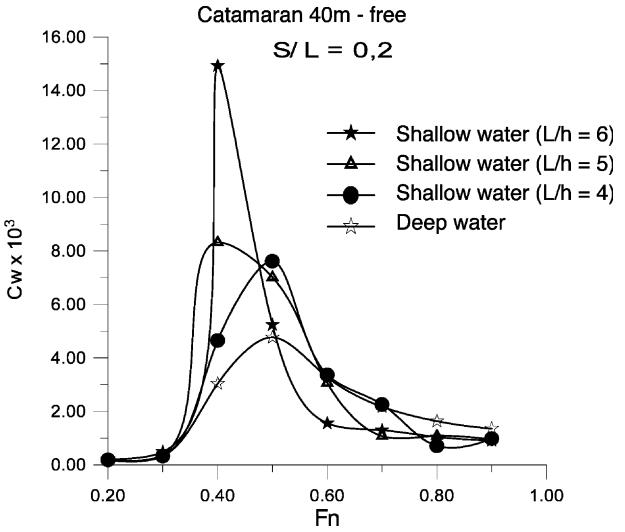

Fig. 23. C_w comparison for $S/L = 0.2$ in different depths of water.

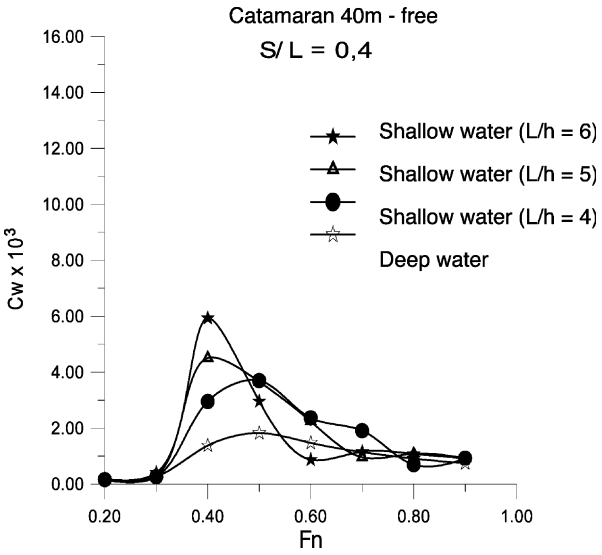

Fig. 24. C_w comparison for $S/L = 0.4$ in different depths of water.

Between Froude number 0.6 and 0.7 wave resistance decreases with decreasing water depth for the whole S/L range.

For Froude numbers lower than 0.3, the results are practically the same for the whole range of S/L and L/h.

Figs. 23 and 24 show that as twin hull separation increases, C_w coefficient achieves the lower value. However, at $L/h < 5$, the C_w coefficient continues to

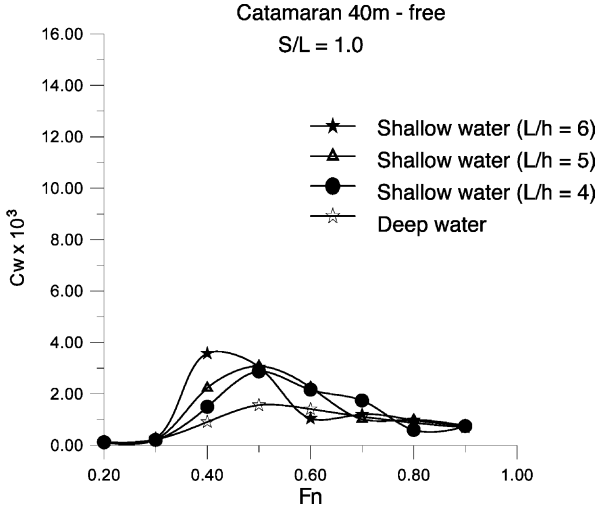

Fig. 25. C_w comparison for $S/L = 1.0$ in different depths of water.

reach the critical value at Froude number 0.4.

Fig. 25 shows the same tendency as Figs. 23 and 24, however, the interference effect between hulls is minor.

As in Millward (1992), a tendency was observed for interference between catamaran hulls to be null at Froude numbers smaller than 0.3 and negative at Froude numbers larger than 0.7, in any depth of water.

Results indicate the tendency for C_w to peak at lower Froude numbers in shallow water. In deep water, critical C_w occurs at Froude number 0.5. When water depth decreases, this critical C_w occurs around Froude number 0.4.

In shallow waters, the effect of hull separation causes critical C_w value to increase significantly.

According to Chengyi (1994), when the distance between hulls is small and the craft speed is high, the flow between hulls tends to suffer the blockage phenomenon. In this case, the surface of the water is lifted in a violent splash. According to test results with catamaran round bottom (arc bilge) hulls and chine bilge hulls, the following expression is used to calculate the Froude number (Fr_b):

$$Fr_b = \sqrt{\frac{10}{\frac{L}{b}\left[\left(\frac{S}{S - C_p b}\right)^2 - 1\right]}} \tag{5}$$

where L is the craft length (m); S the distance between two hull centers (m); b the breadth (m) and C_p the prismatic hull coefficient.

The tests in Chengyi (1994) indicate that the interference between catamaran hulls that causes a reduction in resistance occurs at Froude numbers higher than 0.5 ($Fn > 0.5$).

For different S/b, the Froude number at which negative interference begins — Fr_0 (reduction in resistance)—can be calculated by the following expressions:

$$\begin{aligned}
Fr_0\left(\frac{S}{b} = 1,6\right) &= 0.55 + 0.057\left[\frac{\nabla}{(0,1L)^3}\right]^2 (A)\\
Fr_0\left(\frac{S}{b} = 2,0\right) &= 0.55 + 0.050\left[\frac{\nabla}{(0,1L)^3}\right]^2 (B)\\
Fr_0\left(\frac{S}{b} = 2,6\right) &= 0.55 + 0.046\left[\frac{\nabla}{(0,1L)^3}\right]^2 (C)\\
Fr_0\left(\frac{S}{b} = 3,2\right) &= 0.55 + 0.044\left[\frac{\nabla}{(0,1L)^3}\right]^2 (D)\\
Fr_0\left(\frac{S}{b} \geq 6,0\right) &= 0.55 + 0.042\left[\frac{\nabla}{(0,1L)^3}\right]^2 (E)
\end{aligned} \tag{6}$$

Using the equations proposed by Chengyi (1994) for *blockage* Froude (Fr_b) and

the Froude number where null interference (Fr_0) begins, the following values were calculated for the catamarans analyzed in Figs. 23– 25, respectively.

For Fig. 23 ($S/L = 0.2 - k/b = 2.66$)$\Rightarrow Fr_0 = 0.640$ and $Fr_b = 1.00$.
For Fig. 24 ($S/L = 0.4 - k/b = 5.33$) $\Rightarrow Fr_0 = 0.634$ and $Fr_b = 1.59$.
For Fig. 25 ($S/L = 1.0 - k/b = 13.33$)$\Rightarrow Fr_0 = 0.632$ and $Fr_b = 2.67$.

It was observed that smaller the distance between hulls, the larger the value of Fr_0 and the beginning of negative interference. In the chine hull catamaran case, according to Chengyi (1994), negative interference begins at Froude numbers higher than 0.63.

Results for variation in submerged volume and wetted area were as follows:

The 40-m catamaran submerged volume increases significantly in shallow water and when the interference effect is present. Percentage sinkage is 33% (Fig. 26). The results show that when both effects are present, the resistance increases to a very high value.

In deep water, the effects lead the submerged volume to increase abruptly to 13% ($Fr = 0.5$) and then decrease to 11% at $Fr > 0.6$.

In shallow water, submerged volume fell below the deep water values at $0.6 < Fn < 0.8$.

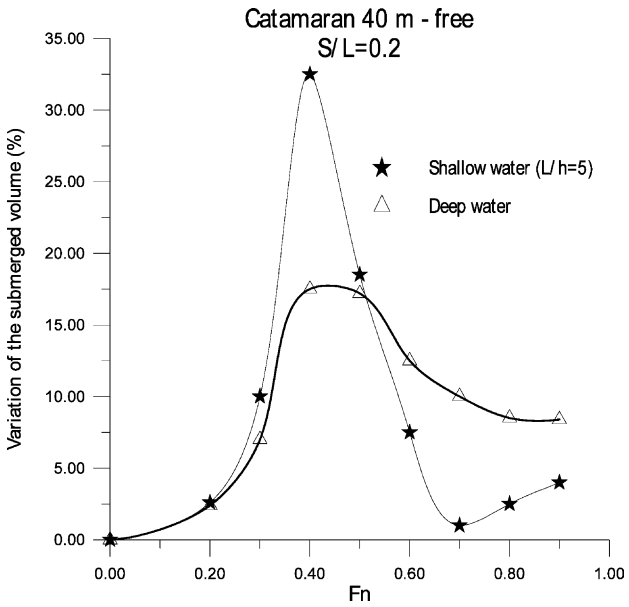

Fig. 26. Forty-meter catamaran submerged volume variation in free condition and $S/L = 0.2$.

The variation in the wetted surface area will be shown for catamaran hull separation (S/L) of 0.2 and 1.0 in shallow water ($L/h = 5$) and deep water (Figs. 27–29).

At low Froude numbers (to approximately 0.3), the variation in wetted surface area is similar in all cases. However, when Froude number reaches 0.4 a substantial increase in the wetted surface area is seen, mainly when the interference between hulls and the shallow water effects occur.

Millward (1992) was used to compare the results generated by the Shipflow™ program, although his study did not contemplate the free craft condition.

The results were expressed in the form of a non-*dimensional* ($C*$) wave resistance coefficient, adopted in Millward (1992)

$$R^* = \frac{R}{(8/\pi)\rho g(b^2T^2/L)} \tag{7}$$

$$C^* = \frac{R^*}{Fn^2} \tag{8}$$

where R is the wave resistance; L the catamaran length (m); b the breadth (m); T the draft (m); ρ the fluid density (kg/m^3); g the acceleration of gravity (m/s^2) and Fn the Froude number.

Figs. 30–35 show that the water depth as well as the distance between catamaran hulls has little influence on the C^* values at Froude numbers smaller than 0.3 and larger than 0.7. For Froude numbers higher than 0.7, there is a convergence of C^* values.

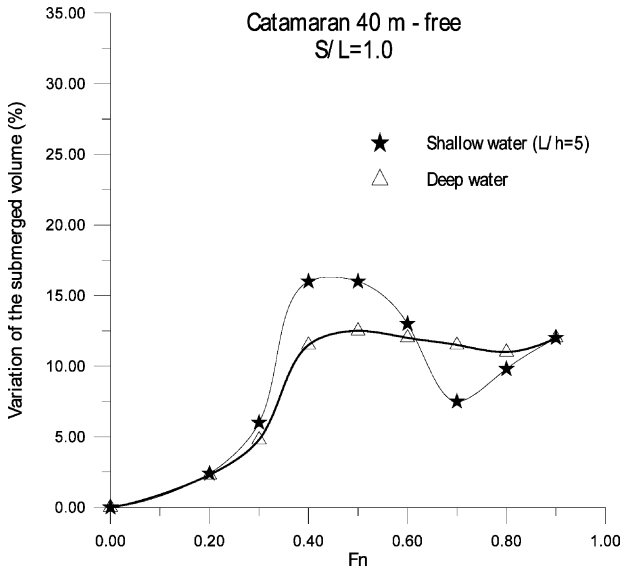

Fig. 27. Forty-meter catamaran submerged volume variation in free condition and $S/L = 1.0$.

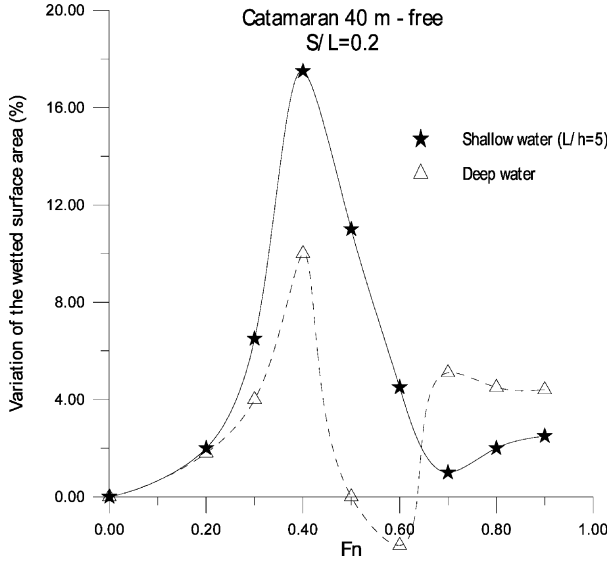

Fig. 28. Forty-meter catamaran wetted surface area variation in free condition and $S/L = 0.2$.

When the C^* results obtained by the Shipflow™ program for the 40-m catamaran are compared with Millward (1992), the shape of the C^* curve is the same and the results are very close.

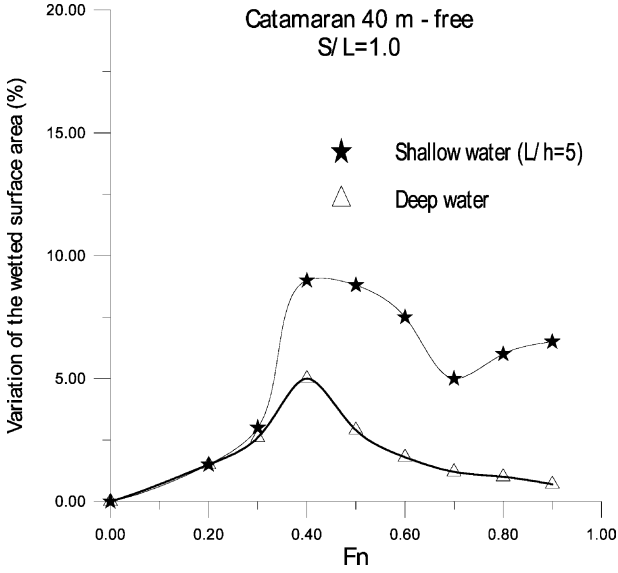

Fig. 29. Forty-meter catamaran wetted surface variation in free condition and $S/L = 1.0$.

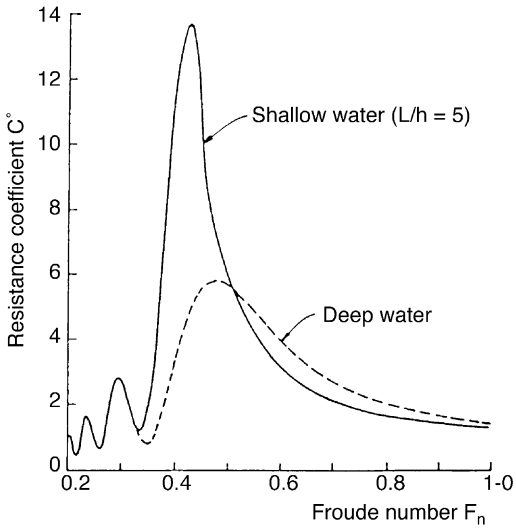

Fig. 30. Catamaran C^* coefficient for $S/L = 0.2$ in shallow and deep water (Millward, 1992).

4.1. Catamaran trim

Catamaran trim was studied for hull separations (S/L) 0.2 and 1.0 in shallow water ($L/h = 5$) and deep water conditions, Doctors (1991). Figs. 36 and 37 show the results in graphic form.

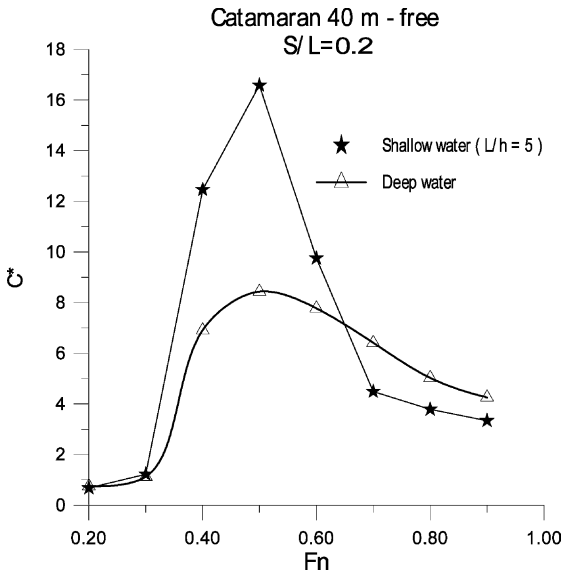

Fig. 31. Catamaran C^* coefficient for $S/L = 0.2$ in shallow and deep water (Shipflow® (1988)).

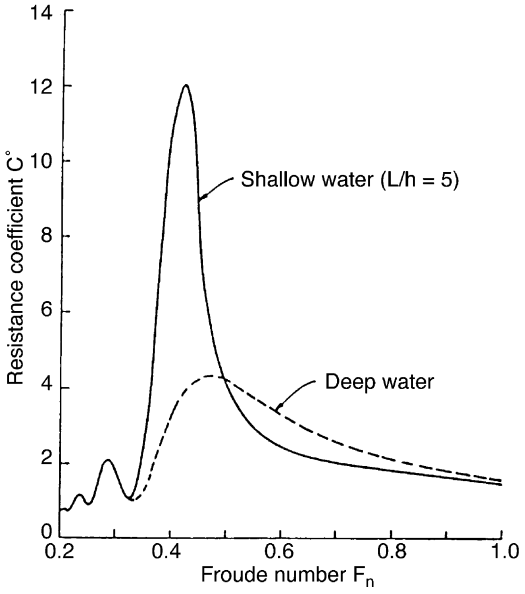

Fig. 32. Catamaran C^* coefficient for $S/L = 0.4$ in shallow and deep water (Millward, 1992).

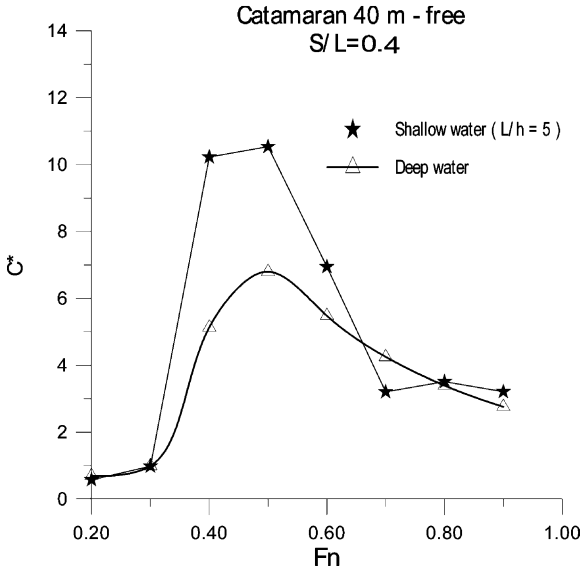

Fig. 33. Catamaran C^* coefficient for $S/L = 0.4$ in shallow and deep water (Shipflow℠).

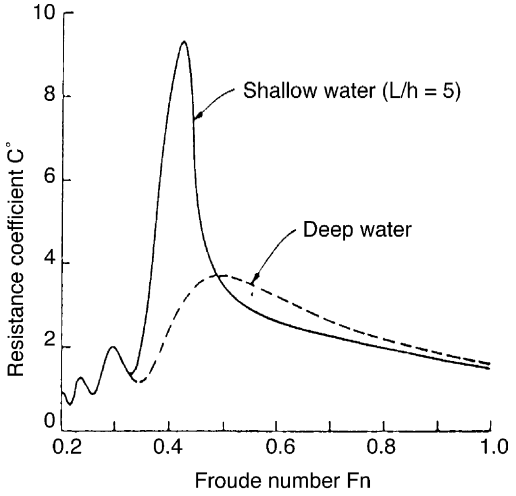

Fig. 34. Catamaran C^* coefficient for $S/L = 1.0$ in shallow and deep water (Millward, 1992).

At Froude numbers up to 0.3, dynamic trim is significant and sinkage is parallel. When the catamaran reached Froude number around 0.4 it gains stern trim with significant variation in draft. Above Froude number 0.5, sinkage happens practically with the same trim angle with small variations.

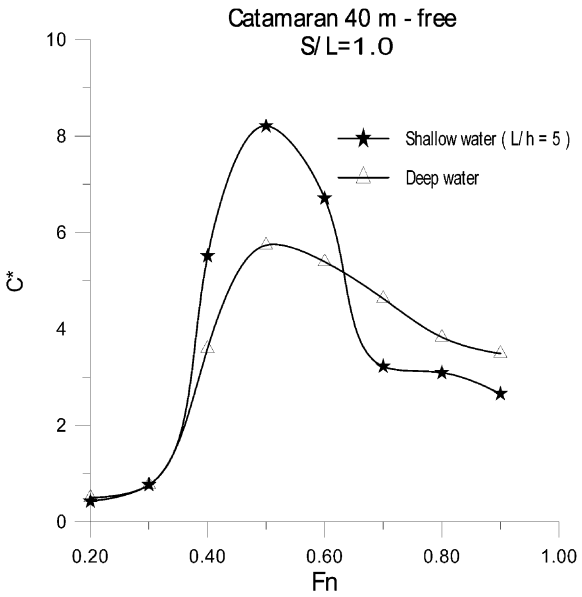

Fig. 35. Catamaran C^* for $S/L = 1.0$ in shallow and deep water (Shipflow™).

Fig. 37 shows the same test in shallow water ($L/h = 5$).

The bottom effect increases dynamic trim as shown in Fig. 37. Comparison with the sinkage in deep water shows that here sinkage is 29% greater.

Above Froude number 0.6, the stern reduces the sinkage reaching draught of approximately 2.3 m, which is practically equal to the value achieved in deep waters (2.4 m). Therefore, it can be concluded that the effect of shallow waters only causes significant variation in sinkage at Froude numbers between 0.4 and 0.6.

4.2. Waves generated by the twin hull

The purpose of analyzing waves generated by the passage of the craft was to ascertain the heights of waves spreading starting from the catamaran hull to a certain distance. Here, the distance was considered as 60% of the hull length.

Fig. 38 shows the positioning of a catamaran hull in plane x–y. The points in the graph represent the center of each panel used to represent the free surface.

Figs. 39–42 reflect a transverse plane showing the elevation of the points of the free surface that define the wave height or elevation of each panel center of the free surface. These points are defined starting from the side of the catamaran hull in deep water and shallow water ($L/h = 5$) conditions with hull spacing $S/L = 0.2$, which is considered to be the most restrictive.

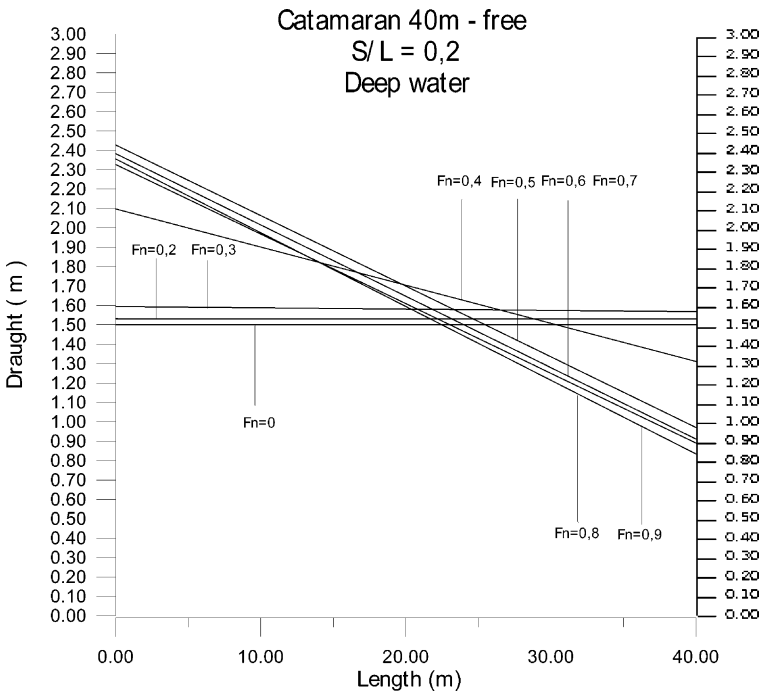

Fig. 36. Trim variation for different Froude numbers ($S/L = 0.2$ and deep water).

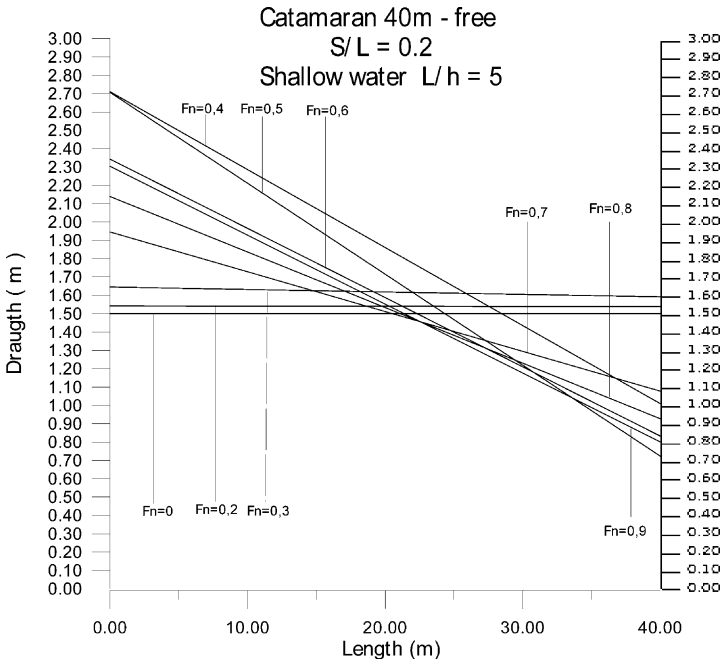

Fig. 37. Trim variation for different Froude numbers ($S/L = 0.2$ $L/h = 5$).

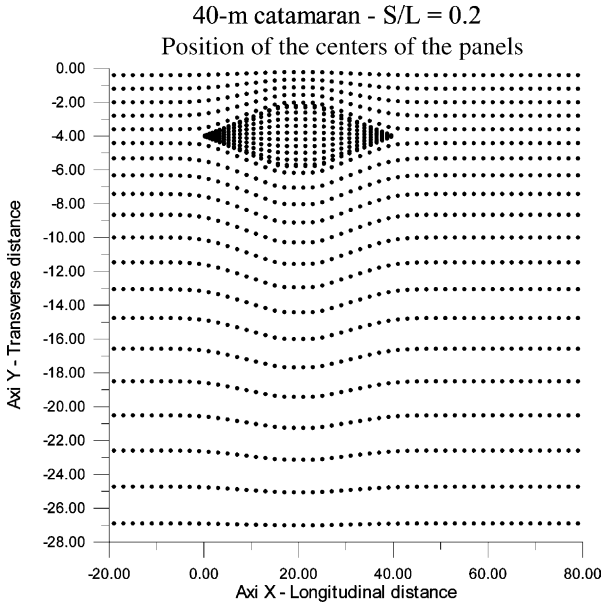

Fig. 38. Position of a 40-m catamaran hull and the free surface.

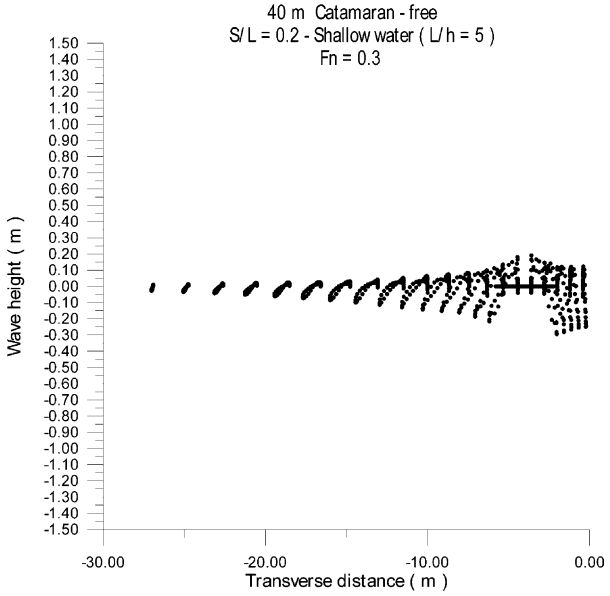

Fig. 39. Wave height generated in shallow water ($L/h = 5$) at $Fn = 0.3$.

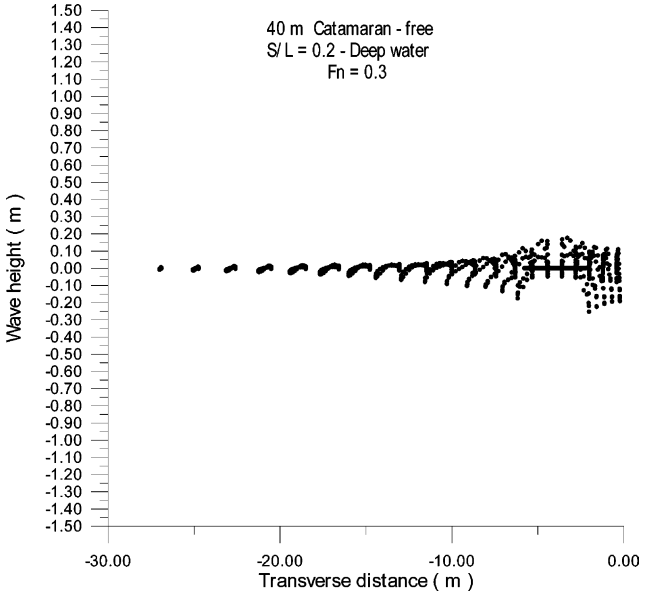

Fig. 40. Wave height in deep water at $Fn = 0.3$.

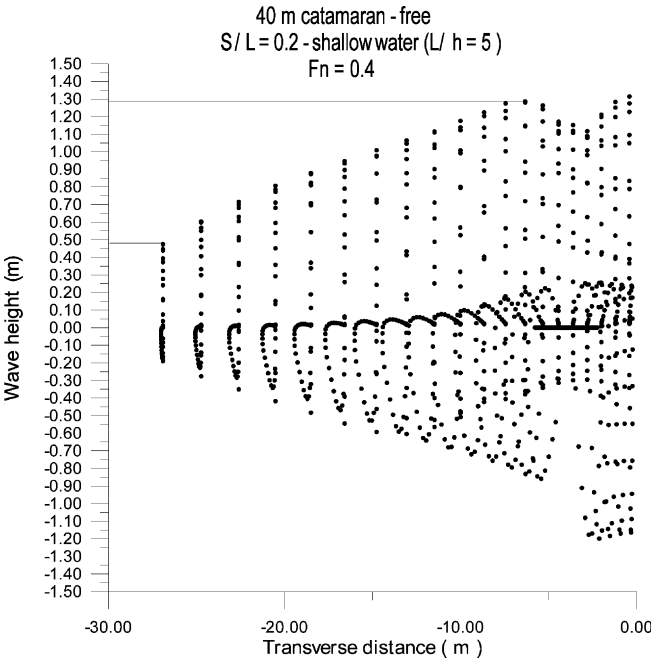

Fig. 41. Wave height in shallow water ($L/h = 5$) at $Fn = 0.4$.

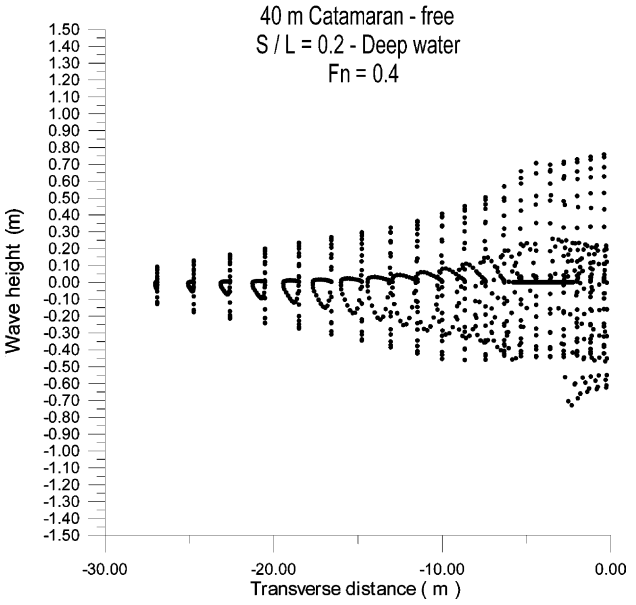

Fig. 42. Wave height in deep water at $Fn = 0.4$.

Figs. 39–42 indicate:

The Shipflow™ program made it possible to calculate the height of the waves generated by the catamaran hull and also to study their effect on the river shore.
The effect of shallow water is very important when considering the height of waves generated by the catamaran hull.

5. Conclusion

The results yielded by 3D theory (Shipflow™) and 2D theory (Slender computer software program) are useful in analyzing the catamaran at a preliminary design stage.

Some conclusions were drawn from catamaran simulation:

For $S/L > 0.6$, no significant effects of interference between the hulls were found and wave resistance can be calculated as for infinitely separated twin hulls.
The type of hull section does not modify wave resistance significantly.
The maximum positive interference occurs around Froude number 0.5 for deep water and 0.4 for shallow water.
Differences between Shipflow™ (1988) and SLENDER program (Williams, 1994) results are high for smaller S/L ratios.
At $0.2 \leq Fn \leq 0.4$ and $Fn > 0.8$, the results obtained by the Shipflow™ and SLENDER programs are very close to those of Millward (1992).
Across the whole S/L range (0.2, 0.4 and 1.0), at Froude numbers above 0.8, values of C_w were observed to converge at around 0.0002.
Also observed was that, at Froude numbers around 0.5, the smaller the spacing between hulls, the greater is the elevation of the C_w curve.
When the effect of shallow waters is present, hull interference is negative at Froude numbers ≥ 0.7.
The effect of hull separation, added to the shallow water effect, causes a significant increase in critical C_w values.
The heights of waves generated by the hull can be studied by Shipflow™. The results can be used to study and minimize the effect at the river shore (Doctors, 1991).

Acknowledgements

The authors would like to thank the Brazilian National Scientific and Technical Development Board (*Conselho Nacional de Desenvolvimento Científico e Tecnológico*, CNPq), Rio de Janeiro Federal University and Pará Federal University for supporting this study.

References

Chengyi, Wang, 1994. Resistance characteristic of high-speed catamaran and its application. Marine Design and Research Institute of China.

Dawson, C.W., 1977. A practical computer method for solving ship wave problems. In: 2nd International Conference on Numerical Ship Hydrodynamics, Berkeley.

Doctors, L.J., 1991. Some hydrodynamic aspects of catamarans. Proc. Inst. Eng., Austr. 16, 295–301.

Everest, J.T., 1968. Some research and hydrodynamics of catamarans and multi-hulled vessels in calm water. Trans. N.E.C.I.E.S. 84, 129–148.

FLOWTECH, 1988. Shipflow™ 2.4, User Manual.

Havelock, T.H., 1934. The calculation of wave resistance. Proc. RS, series A 144.

Hess, J.L., Smith, A.M.O., 1964. Calculation of non-lifting potential flow about arbitrary three-dimensional bodies.

IMO-HSC CODE, 1995. International Code of Safety for High Speed Craft.

Insel, M., Molland, A.F., 1991. An investigation into the resistance components of high speed displacement catamaran. Royal Institution of Naval Architects, Spring Meeting, paper no. 11,1991.

Kostjukov, A., 1977. Wave resistance of a ship near walls. J. Hydromech. 35, 9–13.

Lunde, J.K., 1951. On the linearized theory of wave resistance for displacement ship in steady and accelerated motions. Trans. SNAME 59, 25–85.

Millward, A., 1992. The effect of hull separation and restricted water depth on catamaran resistance. The Royal Institution of Naval Architects.

Millward, A., Sproston, J.L., 1988. The prediction of the resistance of fast displacement hull in shallow water. Royal Institution of Naval Architects, Maritime Technology Monograph, No. 4.

Newman, J.N., 1977. Marine Hydrodynamics. The MIT press, Cambridge, Massachusetts and London, England.

Nishimoto, K., 1998. Semi-deslocamento Aplicando Mecânica dos Fluidos Computacional.

Picanço, H.P., 1999. Resistência ao Avanço: Uma Aplicação de Dinâmica dos Fluidos Computacional. MSc Thesis, COPPE/UFRJ, Rio de Janeiro.

Wigley, W.C.S., 1942. Calculated and measured wave resistance of a series of forms defined algebraically, the prismatic coefficient and angle of entrance being varied independently. Trans. Inst. Naval Arch. 86, 41–56.

Williams, M.A., 1994. Otimização da Forma do Casco de Embarcações Tipo Swath. MSc Thesis, COPPE/UFRJ, Rio de Janeiro.